Functional Correlates of Outer Retina Remodeling in Intermediate Age-Related Macular Degeneration Using Microperimetry

Serena Fragiotta,[1] Eliana Costanzo,[2] Pasquale Viggiano,[2] Daniele De Geronimo,[2] Gianluca Scuderi,[1] Monica Varano,[2] and Mariacristina Parravano[2]

[1]Ophthalmology Unit, "Sapienza" University of Rome, NESMOS Department, St. Andrea Hospital, Rome, Italy
[2]IRCCS Fondazione Bietti, Rome, Italy

Correspondence: Mariacristina Parravano, IRCCS Fondazione Bietti, Via Livenza 3, 00198 Rome, Italy; mcparravano@gmail.com.

Received: July 21, 2021
Accepted: February 28, 2022
Published: March 15, 2022

Citation: Fragiotta S, Costanzo E, Viggiano P, et al. Functional correlates of outer retina remodeling in intermediate age-related macular degeneration using microperimetry. *Invest Ophthalmol Vis Sci.* 2022;63(3):16. https://doi.org/10.1167/iovs.63.3.16

Purpose. To assess the effect of drusen morphometric changes and choroidal vascular modifications on retinal sensitivity (RS) evaluated through microperimetry in intermediate age-related macular degeneration (iAMD).

Methods. A retrospective review of 18 iAMD patients (18 eyes) with a 12-month follow-up was performed. Eye-tracked spectral-domain optical coherence tomography was obtained, with automatic segmentation of the outer retinal layer (ORL) delineating the drusen area from the external limiting membrane to Bruch's membrane and outer nuclear layer (ONL) thickness maps adjusted manually, as needed. Advanced retinal pigment epithelium analysis was also performed with a ZEISS PLEX Elite 900. Microperimetry obtained under mesopic conditions was overlaid with the corresponding thickness maps with Fiji software. The choroidal vascularity index (CVI) was calculated in the subfoveal b-scan and volumetric in the central 1-mm subfield.

Results. A reduced central ONL thickness was strongly associated with RS decline at the same region ($r = 0.69$, $P = 0.002$) and globally ($r = 0.80$, $P < 0.001$) at baseline, but also at 1 year in the central subfield (central: $r = 0.70$, $P = 0.001$). One-year subfoveal CVI variation, differently from volumetric CVI, directly influenced the central ($r = 0.64$, $P = 0.004$) and global RS ($r = 0.59$, $P = 0.009$), indicating that a CVI reduction negatively affected RS. A greater volumetric CVI within central 1-mm was associated with ORL thickening at 1 year ($r = 0.61$, $P = 0.008$).

Conclusions. Progressive degeneration of the ONL is related to irreversible photoreceptor dysfunction in iAMD. Likewise, choroidal vascular modifications are associated with a significant functional decline in the central region and diffusely.

Keywords: drusen remodeling, age-related macular degeneration, microperimetry, drusen regression, spectral-domain optical coherence tomography, retinal sensitivity, choroidal vascularity index

Age-related macular degeneration (AMD) is a progressive disease where the accumulation of drusen/basal linear deposits and/or subretinal drusenoid deposits (SSDs) play a crucial role in the progression to end-stage complications with a substantial loss of retinal pigment epithelium (RPE) and photoreceptors.[1] Drusen dynamic remodeling characterized by growth and formation of new drusen or drusen regression with a reduction in number and volume are part of the physiologic drusen life-cycle leading to macular complications.[2–4] At early stages, the elevated RPE of the drusen is relatively intact, but progressively it becomes thinner and less pigmented, allowing the visualization of drusen as yellowish lesions.[5,6] With time, drusen may fade and disappear, leaving an irregular mottling of the RPE. These changes were initially thought to not account for any functional implications unless pigment epithelium detachment or geographic atrophy occurs.[3] However, it has been widely demonstrated that intermediate AMD exhibits a significant decline of visual function appreciable through microperimetry, particularly by using scotopic or dark adaptation microperimetry, as the rod function is affected first.[7–15]

Microperimetry has provided a more detailed assessment of macular function, and its reproducibility with topographical correspondence is considered an important advantage when measuring functional changes longitudinally.[7,16–18] Microperimetric alterations can be useful in discriminating between early and intermediate AMD stages,[19] as it helps to detect subtle functional changes not demonstrable through a conventional visual acuity test.[12] Despite this, the potential functional impact of drusen dynamic changes, which can be considered part of physiologic remodeling in intermediate AMD, has not, to our knowledge, been investigated using microperimetry.

The present work was devoted to understanding whether and how morphometric changes induced by drusen morphometric modifications and choroidal microvascular

insufficiency impact the cone–rod function as assessed by retinal sensitivity using microperimetry. Particularly, this hypothesis was evaluated by correlating 1-year morphometric changes in the outer retina thickness, including the outer nuclear layer (ONL) and outer retinal layer (ORL) delimiting drusen area, and choroid with retinal sensitivity obtained with mesopic microperimetry in the central 3 mm of eyes with intermediate AMD. Further, we aimed to provide an estimation of drusen remodeling in intermediate AMD over a 1-year follow-up through optical coherence tomography (OCT).

Materials and Methods

This pilot study was a retrospective, observational chart review of patients 50 years of age or older who were graded as stage 3 AMD according to the international grading system for AMD.[20] They were followed for a minimum of 12 months. The study adhered to the tenets of the Declaration of Helsinki and approved by the institutional review board committee at the IRCCS- Bietti Foundation, Rome, Italy.

Inclusion criteria were the presence of complete medical records, fundus autofluorescence (FAF), spectral-domain optical coherence tomography (SD-OCT), optical coherence tomography angiography (OCTA), and fluorescein angiography (FA) or indocyanine green angiography as needed. Exclusion criteria were severe ocular media opacities interfering with the multimodal visualization of the drusen and other significant ophthalmic pathologies.

Eyes with conventional drusen characterized by multiple RPE elevations with variable internal reflectivity on OCT B-scans were analyzed.[21] Reticular pseudodrusen (RPD), also known as subretinal drusenoid deposits (SDDs), were recognized as conical or flat hyperreflective deposits within the RPE and the boundary between the inner and outer segments of photoreceptors, better seen on infrared reflectance.[22] Eyes presenting with a pure RPD/SDD phenotype in the absence of drusen were not considered in the present analysis. The main reasons for this decision reside in the technical limitations in delineating their area, considering their configuration and anatomical locations. Also, RPD/SDDs may affect the mesopic and scotopic retinal sensitivity more profoundly than conventional drusen, leading to a biased interpretation of the results.[23]

Imaging

All patients underwent SD-OCT scans with images obtained using a SPECTRALIS HRA+OCT (Heidelberg Engineering, Heidelberg, Germany). OCT scan patterns were acquired with a minimum of a 20° × 20° rectangle centered on the fovea and 25-line B-scans spaced 235 µm apart and composed of 50 averaged frames. Baseline scans served as reference, and all subsequent images were acquired using a follow-up mode to ensure reproducibility. Segmentation errors were adjusted by a single experienced operator (SF). FAF was also obtained during the same examinations (488-nm excitation, 500- to 680-nm barrier filter light transmission, 30° × 30°) using the SPECTRALIS HRA+OCT. Swept-source OCT angiography (PLEX Elite, Carl Zeiss Meditec, Jena, Germany) was performed using a 6 × 6-mm scan pattern centered on the fovea. The scans were processed through the Advanced RPE analysis tool that calculates the drusen area and volume in the 3-mm and 5-mm circles centered on the fovea.

Microperimetry was performed using the Macular Integrity Assessment system (MAIA; CenterVue S.p.A., Padova, Italy) under mesopic conditions using a customized grid of 33 stimuli around the central 10°, a white background illumination of 4 asb (1.27 cd/m^2), Goldmann III stimuli with a projection time of 200 ms, and a 4-2 staircase strategy. Retinal sensitivity maps (dB) were automatically calculated by the software, which also provided an estimation of the bivariate contour ellipse area (BCEA) encompassing 63% and 95% of fixation points (±1 SD and ± 2 SD, respectively). Microperimetry was performed twice within 1 week to rule out potential learning effects in each patient after a brief training session, and the second test was used for the analysis. Tropicamide 1% was used to dilate the pupil in the selected eye.

Image Analysis

Macular thickness values within the Early Treatment of Diabetic Retinopathy Study (ETDRS) grid were calculated using the automated segmentation provided by the SPECTRALIS software. Each OCT macular cube was segmented using the "All" layers mode, allowing us to obtain two different customized segmentations that were used to calculate the outer retina morphometric remodeling over time. ORL thickness maps were generated by an algorithm segmenting between the outer boundary of the external limiting membrane (ELM) and Bruch's membrane (BrM), not reflecting the anatomical outer retina extending from the outer plexiform layer (OPL) and the RPE. Likewise, the ONL thickness calculated by the OCT software was delineated between the outer boundary of the OPL and the inner boundary of the ELM, corresponding anatomically to the Henle's fiber layer and ONL.[24]

The ORL thickness maps quantitatively estimated the average thickness values (µm) and the volume (mm^2) for each ETDRS quadrant. The changes in ORL maps represented outer retina morphometric modifications from the ELM to BrM and served as an indirect surrogate of drusen changes in terms of average thickness values (µm) and volume (mm^2) between year 1 (Y1) and baseline (Y0) (Fig. 1). The advanced RPE analysis algorithm is a new, validated, automated mechanism for drusen assessment that provides quantitative values for drusen area and volume in the 3-mm and 5-mm circles centered on the fovea (Fig. 1).[25]

Both RPE analysis and calculation of the ORL thickness maps were performed at the initial examination (Y0) and after 1 year of follow up (Y1). However, the ORL thickness and volumetric maps allowed more accurate overlap, with the microperimetry test providing quantitative values of the central ETDRS ring representing the central 1-mm area and the 3-mm parafoveal ring being comprised of four areas: temporal, superior, nasal, and inferior (excluding the central 1 mm). Perifoveal ETDRS rings (6 mm) were excluded from the analysis to allow accurate overlap with the spatial distribution of the projection points of the microperimetric examination (Fig. 2).

The thickness quantitative maps were overlaid with the corresponding microperimetric maps using Fiji software (Fig. 2). Considering the possible variation in stimuli projections on the fundus photographs, the overlaid map was built to obtain the same number of points for each sector considered. The estimation was based on a trend found on

Investigative Ophthalmology & Visual Science

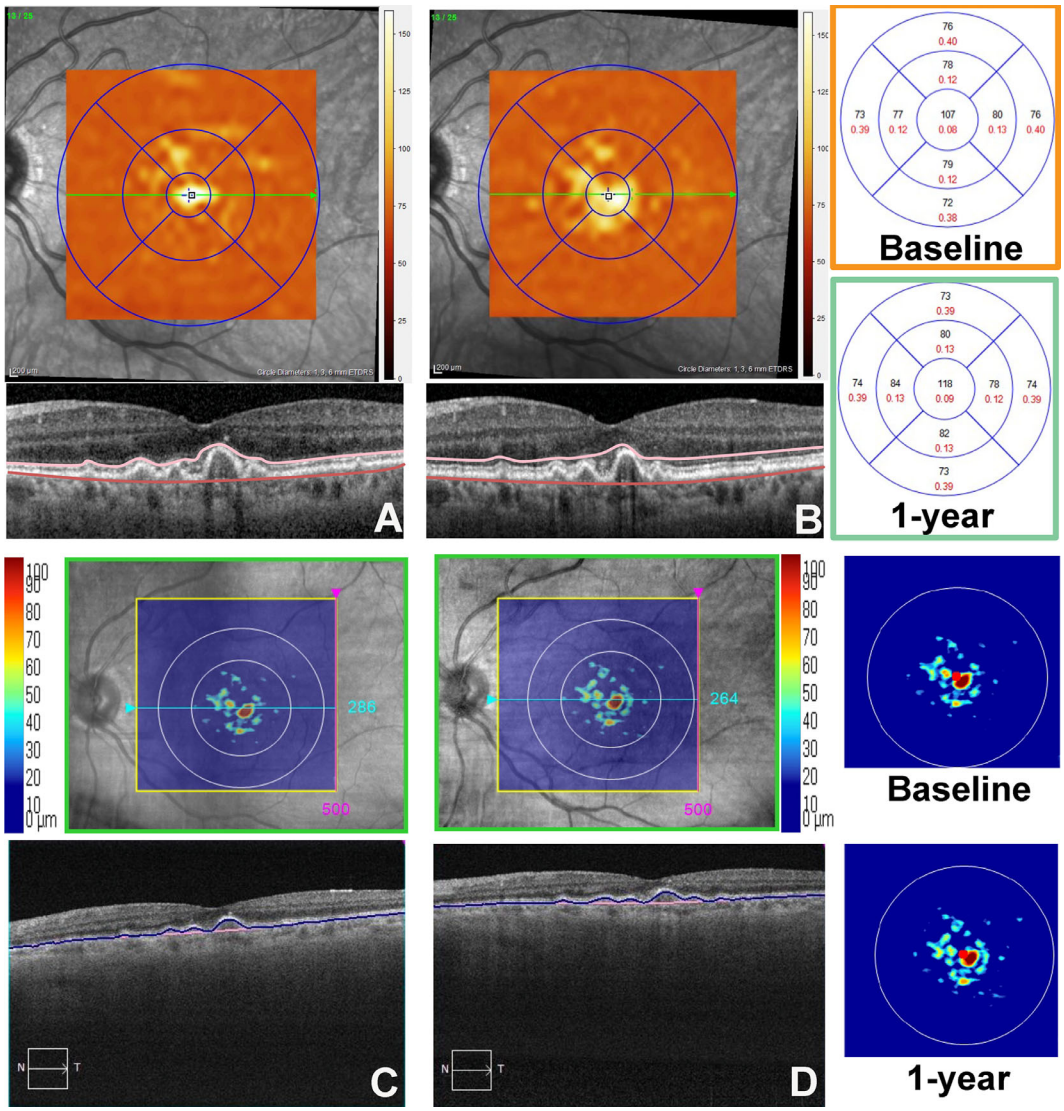

Figure 1. Morphometric analysis of ORLs and drusen. (**A**) Near-infrared with superimposed ORL colorimetric map with ETDRS circle diameters (1, 3, 6 mm) at baseline. The ORL map is delineated between the ELM and BrM, as shown on OCT B-scans. (**B**) ORL thickness map after 1-year follow-up. The insets display the average thickness (mm) and volume (mm^2) at baseline (*orange*) and at 1 year (*green*). (**C**) Advanced RPE analysis obtained using the ZEISS PLEX Elite at baseline. The algorithm measures elevations of the RPE as shown on OCT B-scan segmentation (RPE–BrM). (**D**) Advanced RPE analysis output overlaid on the infrared image after 1 year. The insets (*right*) represent the RPE profile colorimetric map at baseline and at 1-year follow-up.

several images, where the final map contained five points within the central 1-mm subfield and six points for each parafoveal sector (4 parafoveal ETDRS sectors × 6 points each = 24 parafoveal points). Therefore, four points located in the perifoveal sectors were excluded from the analysis; further details are shown in Figure 2.

The choroidal vascularity index (CVI) defines the proportion of the vascular component in the choroid by calculating the ratio of the luminal area compared to the total choroidal area. This index was calculated through post-processing with Fiji 2.1.0/1.53.c[26] using a methodology previously described by Sonoda et al.[27] The CVI was obtained through the subfoveal horizontal B-scan enclosing the parafoveal rings (3 mm in length). Volumetric estimation of the CVI within the central 1-mm subfield for a total of 180 B-scans was performed by applying the Cavalieri principle of stereology analysis, as previously described on adjacent OCT scans.[28–30] In brief, the volume of two adjacent OCT scans, considered as a segment, was determined using the following equation:

$$Vol = d\left(\frac{A_x + A_{x+1}}{2}\right)$$

where *Vol* is the CVI volume within a segment constituted by two consecutive OCT scans (x and $x + 1$); d is the distance between adjacent slices (in µm); A is the CVI area; and x is the OCT scan number. Volumetric CVI was then calculated by summing the volumes of individual segments spanning the central 1-mm on the ETDRS ring; for further details, see Figure 3. If both eyes were eligible, only one eye was randomly selected, generating a random allocation sequence. Even values were assigned to the right eye and

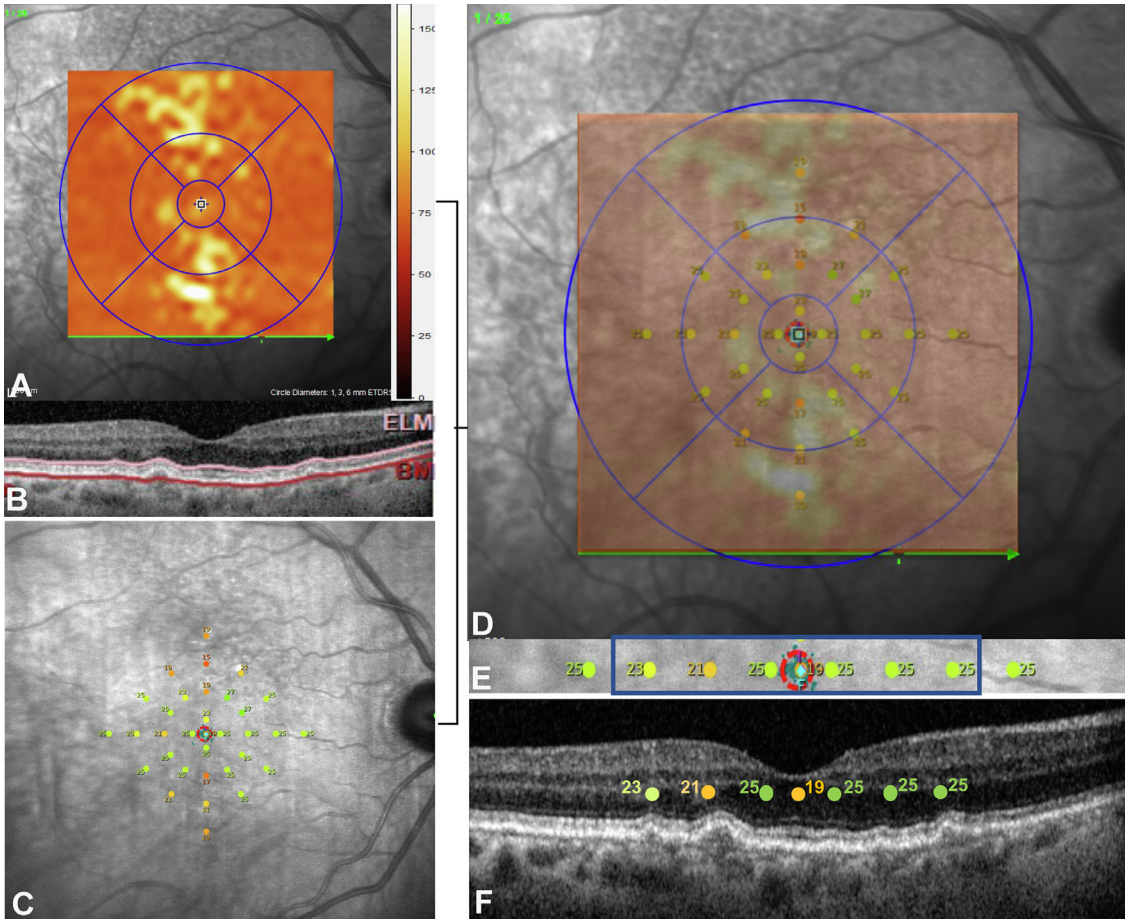

Figure 2. Imaging analysis. (**A**) ORL thickness map obtained using Heidelberg SPECTRALIS software that delineates the drusen profile between the outer boundary of the ELM and BrM, as detailed in **B**. (**C**) Microperimetry examination obtained at baseline under the mesopic condition composed of 33 points projected on the central 10°. The microperimetry examination was overlaid (using Fiji 2.1.0/1.53.c) on near-infrared reflectance using the ETDRS map as a reference to analyze the 1-mm central subfield and parafovea. Perifoveal ETDRS rings (6 mm) were subtracted from the analysis to allow an optimal overlap between microperimetric examination and thickness maps. (**E**) Retinal sensitivity points analyzed in the central 3 mm (enclosed in the *blue rectangle*) and (**F**) their projection on subfoveal OCT B-scans.

odd values to the left eye using an online random sequence generator.

Statistical Analysis

The quantitative variables were expressed as mean ± standard deviation The normality of distribution was verified through the Shapiro–Wilk test. Paired *t*-tests or the Wilcoxon test were used to calculate differences within the same population. Unpaired *t*-tests or the Mann–Whitney *U* test were used to assess differences between groups at a given time point. Spearman's rank correlation coefficient was calculated to determine the relationships between variables. The delta difference refers to the net change between the final thickness values and the initial value (delta = $\text{final}_{\text{thickness}} - \text{initial}_{\text{thickness}}$). The absolute value, $|x|$, is the value with regard to its sign (absolute change = $|\text{final}_{\text{thickness}} - \text{initial}_{\text{thickness}}|$). The power analysis for Spearman's rank correlation was conducted in G-POWER 3.1.9.6[31] using an alpha of 0.05 and a power of 0.80 for a two-tailed test. Because Spearman's rank correlation is computationally identical to Pearson's product–moment coefficient, power analysis was conducted using the protocol for estimating power for Pearson's correlation. A Spearman's rank correlation coefficient with 18 participants would be sensitive to effects of $r = 0.60$. This means the study would not be able to reliably detect correlations smaller than $r = 0.60$. All calculations were carried out using SPSS 26.0.0.0 (IBM, Chicago, IL).

Results

A total of 18 eyes of 18 consecutive patients (11 females and seven males) with a mean age of 68.4 ± 8.6 years were included in the present study. No significant changes in terms of best-corrected visual acuity, retinal thickness (ORL and ONL maps), drusen volume (mm^2), retinal sensitivity, BCEA at 63% and 95%, and CVI were identified in the overall population at 1-year follow-up, as outlined in Supplementary Material 1. The mean retinal sensitivity change in the overall population was −0.22 dB/y (95% confidence interval [CI], −0.85 to 0.41). The mean ORL delta change% at 1 year was 5%(95%CI: −0.11 to 0.21), which was significantly greater in terms of mean absolute change (19%, 95%CI:0.03–0.34; Wilcoxon test $P = 0.0002$) in the central 1 mm. In the parafovea region, the 1-year mean dynamic remodeling (delta%) was 1% (95% CI, −0.03 to 0.05; $P = 0.53$ compared to central region), significantly lower than the mean

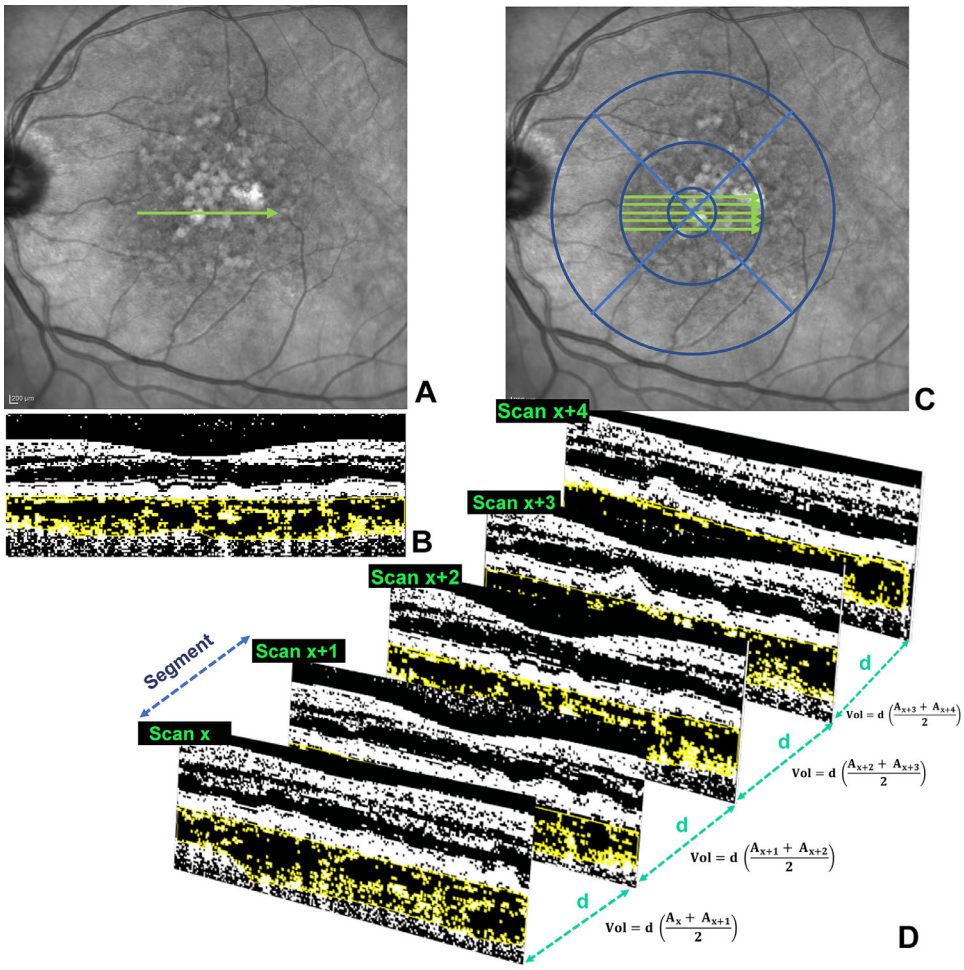

Figure 3. CVI calculation. (**A**) Subfoveal CVIs were calculated on the subfoveal scans enclosing the parafovea (3-mm in length). (**B**) CVIs were obtained through post-processing with Fiji 2.1.0/1.53.c; the *yellow area* covered the total choroidal area considered for the analysis. The index calculates the ratio of the luminal area compared to the total choroidal area. (**C**) Volumetric CVIs were calculated on five consecutive OCT B-scans within the central 1-mm subfield at each follow-up time by applying the Cavalieri principle of stereology analysis. (**D**) Two adjacent OCT B-scans represent a segment. The volume is calculated on a segment using the equation reported (*right side*), which considered the distance (*d*) between scans and the CVI area between two consecutive B-scans (x and $x + 1$). The volumes calculated on each segment were summed to obtain the entire volume of the luminal and total choroidal area to calculate the CVIs.

absolute change (4.8%; 95% CI, 0.01–0.09; $P = 0.01$). However, the absolute net change was greater within the central region than parafovea (−14%; $P = 0.005$). The drusen area calculated within 3 mm showed a significant increase at 1 year ($P = 0.04$) (Fig. 4). Subfoveal and volumetric 1-mm CVIs were similar at baseline ($P = 0.62$) but differed at last follow-up ($P = 0.02$) and in terms of delta changes ($P = 0.03$) at 1 year.

Associations Between Morphometric Factors and Functional Parameters

The variation (delta) of the central (1 mm) ORL thickness was associated with variation in retinal sensitivity in the central subfield ($r = -0.51$, $P = 0.03$). Likewise, the delta changes in drusen area at 3 mm was associated with final central retinal sensitivity ($r = -0.50$, $P = 0.03$) and CVI variation ($r = -0.51$, $P = 0.03$); the same was true for delta volume at 3 mm and central retinal sensitivity at 1 year ($r = -0.48$, $P = 0.04$). However, the reliability of these correlations is uncertain, as the smallest effect size was a correlation coefficient cutoff of $r = 0.60$.

The baseline central ONL thickness was directly associated with final retinal sensitivity in the corresponding central subfield (Spearman's rho, $r = 0.69$, $P = 0.002$), nasal parafovea ($r = 0.67$, $P = 0.002$), and global retinal sensitivity ($r = 0.80$, $P < 0.001$). Central ONL thickness at 1 year demonstrated a strong association with both central ($r = 0.86$, $P < 0.001$) and global ($r = 0.84$, $P < 0.001$) retinal sensitivity, as shown in Figure 4. These associations indicate that ONL thinning in the central 1-mm subfield is directly associated with a decline in retinal sensitivity in the same subfield, but it also influences global retinal sensitivity. This direct relationship is particularly evident at 1-year follow-up (Fig. 4).

Subfoveal delta CVI variation was directly associated with final central sensitivity (Spearman's rho, $r = 0.64$, $P = 0.004$) and global retinal sensitivity ($r = 0.59$, $P = 0.009$), indicating that a reduced subfoveal CVI overtime reflects a decline of function at 1 year. These findings were also corroborated by the evidence of a direct association between delta

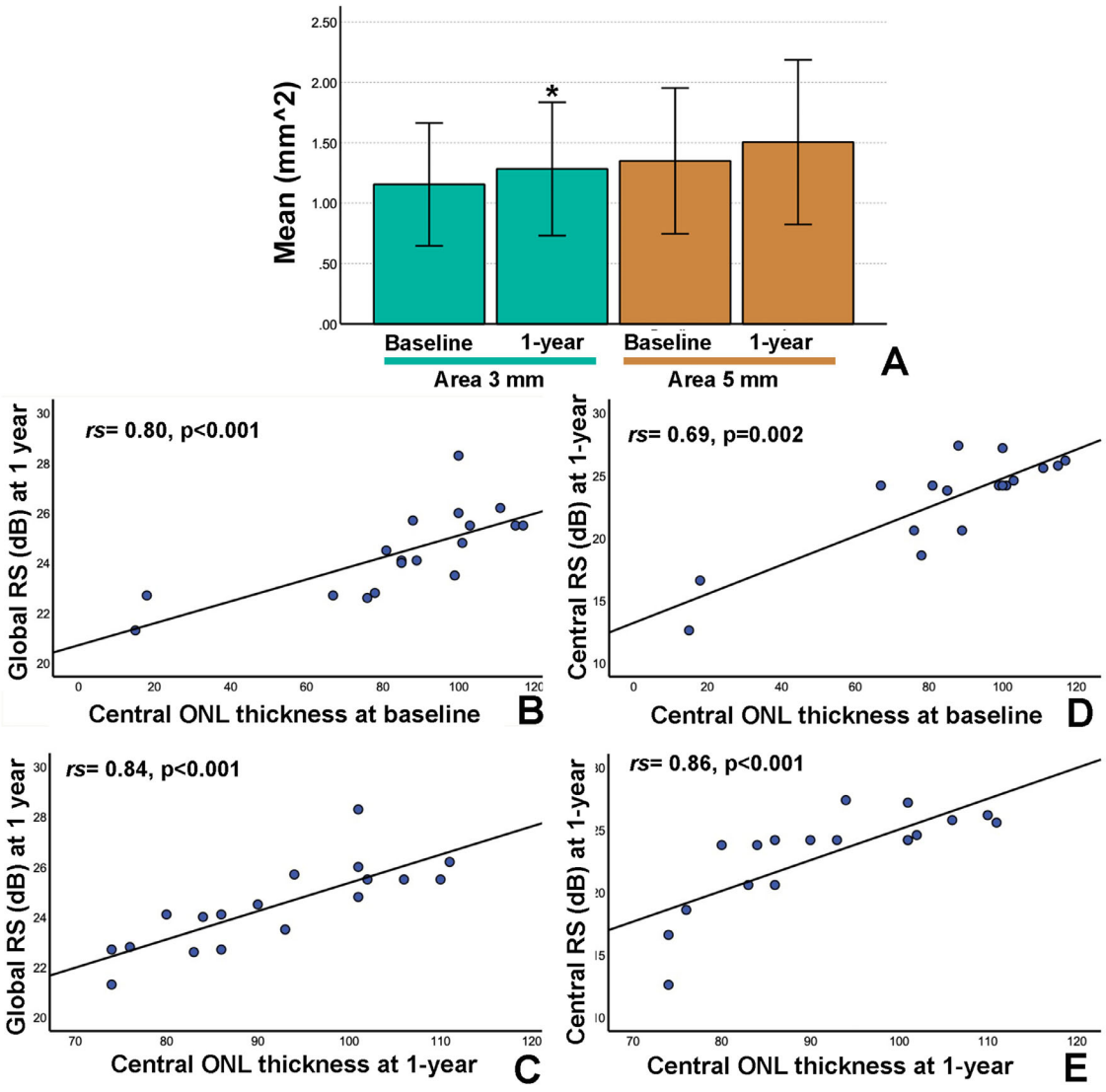

Figure 4. Influence of changes in drusen area and ONL thickness on retinal sensitivity. (**A**) Bar graph showing changes in drusen area within 3 mm and 5 mm at baseline and at 1 year (*$P < 0.05$). *Error bars* represent standard error of the mean (SEM). Scatterplots demonstrate that global retinal sensitivity variation at 1 year was directly influenced by central ONL thickness (1 mm) at baseline (**B**) and at 1 year (**C**) as determined by Spearman's rank correlation coefficient (r). Likewise, global retinal sensitivity at 1 year was directly associated with central ONL thickness (1 mm) at baseline (**D**) and after 1 year (**E**).

subfoveal CVIs and delta global retinal sensitivity ($r = 0.70$, $P < 0.001$). Moreover, subfoveal CVI variation was highly associated with a greater parafoveal net change in retinal sensitivity ($r = -0.80$, $P < 0.001$). Scatterplots of the significant correlations between subfoveal CVIs and retinal function, expressed as retinal sensitivity, are shown in Figure 5.

The analysis of the volumetric CVI calculated within the central B-scans spanning a 1-mm circle (Fig. 3) demonstrated that a greater baseline volumetric CVI was related to a larger central ORL thickness at the last visit ($r = 0.61$, $P = 0.008$). A greater volumetric CVI at baseline was also associated with a larger ORL central subfield change in terms of absolute values ($r = 0.64$, $P = 0.004$). Likewise, a greater CVI at 1 year was associated with a larger ORL absolute change in the parafovea ($r = 0.64$, $P = 0.005$). Figure 5 displays scatterplots showing the associations between volumetric CVI and ORL average thickness, reflecting drusen morphometric changes.

Subanalysis of Morphofunctional Variations According to Drusen Remodeling

An ORL net reduction, indicating drusen resorption, was observed in eight of 18 eyes (44.4%; four males and four females) with a mean age of 68.4 ± 8.45 years, and drusen growth was observed in 10 of 18 eyes (55.5%; seven females and three males) with a mean age of 68.4 ± 9.18 years. Patients were homogeneous for the demographic characteristics of age ($P = 0.69$) and gender ($P = 0.38$). The rate of ORL change in the central subfield at 1 year was −12% (−16.25 µm, $P = 0.89$), whereas eyes with ORL thickening presented a significant percentage change of +18.3% (+17.3 µm, $P = 0.005$). Eyes with ORL thinning presented a greater delta difference in global retinal sensitivity (−0.81 dB/y; 95% CI, −1.9 to 0.29) than eyes with ORL thickening (0.26 dB/y; 95% CI, −0.49 to 1.01; $P = 0.04$). This

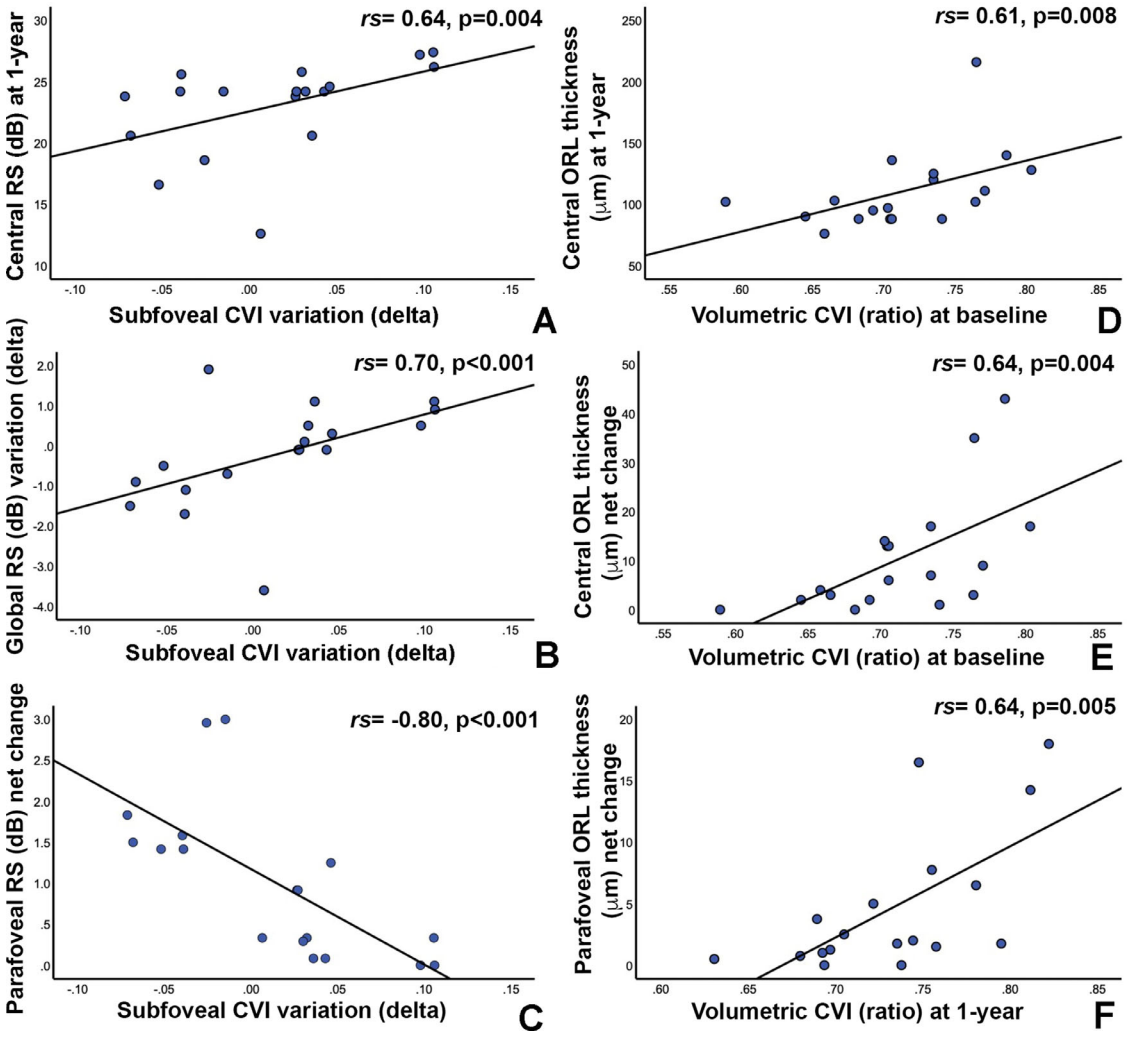

Figure 5. Spearman's rank correlation coefficient (*r*) was used to assess the associations among CVIs, retinal sensitivity, and ORLs. Subfoveal CVI variation (delta) influenced (**A**) central retinal sensitivity at 1 year and (**B**) global retinal sensitivity variation (delta) and negatively influenced (**C**) parafoveal retinal sensitivity net changes in terms of absolute values. Volumetric CVIs at baseline correlated with (**D**) final central ORLs thickness and (**E**) central ORL thickness net changes, whereas volumetric CVI at 1 year was associated with (**F**) parafoveal ORL thickness net variation.

difference was not statistically significant when considering the 0.01 level (two-tailed). In eyes with drusen resorption, the central region corresponded to a greater loss of retinal sensitivity (−1.5 dB/y; 95% CI, −3.32 to 0.33) compared to eyes with drusen growth (0.5 dB/y; 95% CI, −0.46 to 1.46; $P = 0.02$).

Discussion

The present study investigated retinochoroidal morphometric factors associated with retinal sensitivity decline by using topographical correspondence within the central and parafoveal ETDRS regions. Drusen are dynamic elements that can exhibit growth with the formation of new drusen and/or regress over time, leaving ultrastructural modifications of the RPE and photoreceptors.[2] Less commonly, drusen can disappear without leaving residual changes.[3,32] On histopathology, two distinct regression patterns have been described as characterized by gradual fading with a loss of material, leading to a moth-eaten appearance, especially in younger patients. In older patients, the hyalinized amorphous content tends to become coarsely granular with degenerative changes in the RPE.[33]

Smith and coworkers[2] defined dynamic drusen activity as creation plus resorption, which they estimated over a 2-year interval using semi-automated digital analysis applied to color fundus photographs. The authors argued that, as the total dynamic changes were more remarkable than absolute change (|new drusen – resorbed drusen|), it may indicate that creation and resorption are not simultaneous. The model considered a 6-mm region cropped after registration with the major retinal vessels on the color fundus photographs. In contrast, in the present study, the net change is referred to as a thickness change in the drusen area of each ETDRS subfield, with the greatest change evident in the central 1-mm. The thickness approach in estimating drusen change may reveal more accurately the different degrees of drusen regression and growth on a vertical plane with respect to BrM. Therefore, the net change results from a balance between different evolution-

Investigative Ophthalmology & Visual Science

ary stages, with drusen thickening or thinning usually dominant within the same eye. However, the use of advanced RPE analysis suggests promising results in terms of predicting morphofunctional variations in the 3-mm area but should be confirmed in larger studies with a longer follow-up.

The association between ONL thickness and retinal sensitivity in our cohort was consistent with the previous literature, demonstrating that photoreceptor loss is directly proportional to ONL thinning. The progressive decline of ONL is considered to be the result of physical displacement induced by drusen that can contribute to photoreceptor degeneration.[34] Another possible explanation is neural remodeling occurring after photoreceptor degeneration. Loss of rod cells stimulates the recruitment of microglia in the outer nuclear layer, resulting in generalized cell killing and the formation of glial sealing, cell migration, neural loss, and rewiring. The cellular loss also involves rod bipolar and horizontal cells.[35–37]

Histopathological correlates of geographic atrophy confirmed the presence of ONL thinning corresponding with atrophic zone locations.[38] The association of ONL with retinal sensitivity has already been reported in eyes with intermediate AMD, supporting the suggestion that ONL thickness represents a possible surrogate of cone–rod dysfunction.[39,40] The progressive ONL thinning was recently considered to be a predictive factor for conversion toward geographic atrophy or macular neovascularization, with faster thinning in the atrophic progressors.[41]

Another mechanism is represented by gradual vascular impairment associated with the extension of drusen and other sub-RPE deposits, with choriocapillaris degeneration being observable from the onset of AMD.[42,43] It has been suggested that choriocapillaris ischemic changes represent one of the main pathogenetic mechanisms resulting in later macular complications.[44–47] Recently, choriocapillaris flow deficits were shown to be associated with reduced retinal sensitivity as revealed through scotopic microperimetry.[48] Because estimation of choriocapillaris flow voids may suffer from overlying structural changes, such as drusen, that may attenuate the OCTA signal, the accuracy and validity of such an approach are still under debate.[49] Alternatively, other OCT parameters have been largely used to assess choroidal microvasculature status. These parameters include choroidal thickness and the newer CVI, which has demonstrated high reproducibility and validity in estimating pathophysiological variations of the human choroid.[50–52]

In our series, subfoveal CVI variations are directly associated with retinal sensitivity changes, indicating that the modifications of choroidal vasculature reflect a progressive photoreceptor dysfunction as AMD progresses. Agrawal and coworkers[53] demonstrated the usefulness of subfoveal CVI as a reliable indicator of the choroidal status of the entire posterior pole. Accordingly, our findings are relevant to characterizing the CVI parameter with the greatest impact on retinal sensitivity and thus valuable for future larger predictive studies.

The analysis of volumetric CVI within the central 1 mm correlated with variations of ORL, reflecting drusen status but not retinal sensitivity; a greater volumetric CVI was associated with a larger drusen thickness. This preliminary result may indicate that dilated choroidal tissue at baseline could precede drusen growth at 1 year, whereas choroidal thinning anticipates drusen regressive changes at 1 year. This is further supported by the previous evidence that choroidal modifications measured through CVI demonstrate a biphasic trend with an initial thickening, followed by a decreasing thickness in a second phase with AMD progression.[50]

Active remodeling of drusen may be accompanied by both drusen growth and regression at different locations within the same eye.[54] For this reason, in our series, patients were divided into two different subgroups according to drusen growth and regression, using as reference the volumetric thickness map in the central subfield, where the greatest mean difference thickness change between groups was appreciated (−33.4 µm/y). Our preliminary findings may indicate that drusen resorption may be accompanied by a significant decline of retinal sensitivity compared with drusen growth. These hypotheses need to be confirmed in a larger sample and possibly with a scotopic approach in performing microperimetry. In fact, scotopic microperimetry is considered superior to mesopic exams for evaluating the function of rods in intermediate AMD, which may precede cone impairment in the early stages of AMD, especially in the parafoveal regions.[11,54–56] However, cone-mediated central pre-ganglionic element dysfunction has been demonstrated to accompany rod dysfunction, mainly at the foveal and parafoveal locations in the early stages of AMD.[57–60] The topographic correspondence of visual dysfunction within the central 3-mm diameter of the macula was recently demonstrated through a novel biomarker reflecting the slow return to retinal sensitivity following a bright stimulus, the so-called delayed rod-mediated dark adaption. The contradiction with regard to the central regional relationship of rod-mediated dysfunction has been explained as compromised transport through the choriocapillaris and BrM being more prominent in this anatomical location, thus affecting the retinoid resupply route.[24,61]

The longitudinal change of mesopic sensitivity in intermediate AMD was between −0.35 and −0.42 dB/y in previously published reports,[12,40] similar to the results obtained in our overall population analysis (−0.22 dB/y). However, when analyzing eyes with drusen resorption, the global retinal sensitivity reduction was more pronounced (−0.81 dB/y), particularly when analyzing the central 1-mm region (−1.5 dB/y) and the temporal parafovea (−1.13 dB/y). The negative association between drusen volume and retinal sensitivity for both mesopic and dark-adapted microperimetry was recently demonstrated, highlighting the possible structural changes induced by drusen volume.[62] However, this evaluation did not consider the dynamic changes characterizing the drusen lifecycle as did our study; thus, our results can contribute to our understanding of how structural changes over time progressive and affect the integrity of the photoreceptor band known to be related with retinal sensitivity measured through microperimetry.

Recent evidence has shown that microperimetric sensitivity and low luminance deficits are poor predictors for AMD progression by themselves when analyzing patients with large drusen, especially when comparing these findings with the presence of pigmentary on fundoscopy.[63,64] This may be consistent with making a distinction between growth and regression as two different parts of the drusen life-cycle. Pigmentary changes seen on fundus examination may result from profound RPE–basal lamina alterations, with a loss of overlying photoreceptor bands and associated hypertransmission on OCT B-scans,[46] possibly coexisting with some degree of fading or regression of drusen elements.

Limitations of the present study include its retrospective nature, the small sample size, and the relatively short time interval of 1 year that may limit the detection of a

significant drusen remodeling, including the development of macular complications. Another limitation related to the retrospective design is represented by the density of the OCT pattern (25 lines spaced 235 µm), which may underestimate subtle changes in drusen volume. The small cohort size and the relatively short follow-up may account for the large inter-individual differences and small intra-individual changes over time. With a large sample size, it would be interesting to explore whether differences exist among different drusen subtypes, particularly by considering the role of RPD/SDDs as a covariate. In addition, it is possible that the use of scotopic microperimetry could have revealed more interesting insights on functional variations in response to drusen modifications. Despite these limitations, our results confirm that ONL thickness represents a surrogate biomarker of cone–rod impairment, reflecting cone functionality as detected through microperimetry. Moreover, the choroidal fluctuations follow changes in retinal sensitivity, indicating that the choroidal vascular status is an integral part of a degenerative process that occurs before late complications with a significant functional impact. Drusen regression is a physiological end-stage of the drusen lifecycle that can produce fatal photoreceptor damage and/or RPE impairment with detectable photoreceptor dysfunction before macular complications development. Therefore, this evolutionary stage may deserve more careful monitoring and attention. All of the different methods used to evaluate drusen changes over time indicate that most structural–functional variations occur in the central region between 1 and 3 mm. The most important morphological parameter associated with a functional decline is central outer nuclear thickness, but central ORL and drusen area within 3 mm also seem to be promising indicators. More interestingly, choroid vascularity influenced the morphometric variations of the outer retina and even retinal sensitivity. Further studies are essential to determine whether or not early functional alterations may predict morphological and functional prognosis.

Acknowledgments

Supported by the Italian Ministry of Health and Fondazione Roma. SF received the support of Projects to Start Research-Type 2 provided by Sapienza University (2021; protocol number AR22117A81528669). The funders had no role in the study design, data collection and analysis, decision to publish, or preparation of the manuscript.

Disclosure: **S. Fragiotta**, None; **E. Costanzo**, None; **P. Viggiano**, None; **D. De Geronimo**, None; **G. Scuderi**, None; **M. Varano**, Allergan (F), Novartis (F), Bayer (F), Sifi (F); **M. Parravano**, Allergan (F), Novartis (F), Bayer (F), Zeiss (F), Omikron (F), Alfaintes (F), Sifi (F)

References

1. Curcio CA. Soft drusen in age-related macular degeneration: biology and targeting via the oil spill strategies. *Invest Ophthalmol Vis Sci*. 2018;59:AMD160–AMD181.
2. Smith RT, Sohrab MA, Pumariega N, et al. Dynamic soft drusen remodelling in age-related macular degeneration. *Br J Ophthalmol*. 2010;94:1618–1623.
3. Gass JD. Drusen and disciform macular detachment and degeneration. *Arch Ophthalmol*. 1973;90:206–217.
4. Zhang Y, Wang X, Godara P, et al. Dynamism of dot subretinal drusenoid deposits in age-related macular degeneration demonstrated with adaptive optics imaging. *Retina*. 2018;38:29–38.
5. Kim DY, Loo J, Farsiu S, Jaffe GJ. Comparison of single drusen size on color fundus photography and spectral-domain optical coherence tomography. *Retina*. 2021;41:1715–1722.
6. Chen L, Messinger JD, Sloan KR, et al. Abundance and multimodal visibility of soft drusen in early age-related macular degeneration: a clinicopathologic correlation. *Retina*. 2020;40:1644–1648.
7. Hsu ST, Thompson AC, Stinnett SS, et al. Longitudinal study of visual function in dry age-related macular degeneration at 12 months. *Ophthalmol Retina*. 2019;3:637–648.
8. Thompson AC, Luhmann UFO, Stinnett SS, et al. Association of low luminance questionnaire with objective functional measures in early and intermediate age-related macular degeneration. *Invest Ophthalmol Vis Sci*. 2018;59:289–297.
9. Fragiotta S, Carnevale C, Cutini A, Vingolo EM. Correlation between retinal function and microstructural foveal changes in intermediate age related macular degeneration. *Int J Retina Vitreous*. 2017;3:8.
10. Vujosevic S, Pucci P, Casciano M, et al. Long-term longitudinal modifications in mesopic microperimetry in early and intermediate age-related macular degeneration. *Graefes Arch Clin Exp Ophthalmol*. 2017;255:301–309.
11. Wu Z, Guymer RH, Finger RP. Low luminance deficit and night vision symptoms in intermediate age-related macular degeneration. *Br J Ophthalmol*. 2016;100:395–398.
12. Wu Z, Ayton LN, Luu CD, Guymer RH. Longitudinal changes in microperimetry and low luminance visual acuity in age-related macular degeneration. *JAMA Ophthalmol*. 2015;133:442–448.
13. Steinmetz RL, Haimovici R, Jubb C, Fitzke FW, Bird AC. Symptomatic abnormalities of dark adaptation in patients with age-related Bruch's membrane change. *Br J Ophthalmol*. 1993;77:549–554.
14. Owsley C, Jackson GR, White M, Feist R, Edwards D. Delays in rod-mediated dark adaptation in early age-related maculopathy. *Ophthalmology*. 2001;108:1196–1202.
15. Owsley C, McGwin G, Jr, Clark ME, et al. Delayed rod-mediated dark adaptation is a functional biomarker for incident early age-related macular degeneration. *Ophthalmology*. 2016;123:344–351.
16. Parravano M, Oddone F, Tedeschi M, et al. Retinal functional changes measured by microperimetry in neovascular age-related macular degeneration patients treated with ranibizumab. *Retina*. 2009;29:329–334.
17. Grenga PL, Fragiotta S, Meduri A, Lupo S, Marenco M, Vingolo EM. Fixation stability measurements in patients with neovascular age-related macular degeneration treated with ranibizumab. *Can J Ophthalmol*. 2013;48:394–399.
18. Acton JH, Greenstein VC. Fundus-driven perimetry (microperimetry) compared to conventional static automated perimetry: similarities, differences, and clinical applications. *Can J Ophthalmol*. 2013;48:358–363.
19. Cocce KJ, Stinnett SS, Luhmann UFO, et al. Visual function metrics in early and intermediate dry age-related macular degeneration for use as clinical trial endpoints. *Am J Ophthalmol*. 2018;189:127–138.
20. Ferris FL, 3rd, Wilkinson CP, Bird A, et al. Clinical classification of age-related macular degeneration. *Ophthalmology*. 2013;120:844–851.
21. Spaide RF, Curcio CA. Drusen characterization with multimodal imaging. *Retina*. 2010;30:1441–1454.
22. Zweifel SA, Spaide RF, Curcio CA, Malek G, Imamura Y. Reticular pseudodrusen are subretinal drusenoid deposits. *Ophthalmology*. 2010;117:303–312.e1.

23. Corvi F, Pellegrini M, Belotti M, Bianchi C, Staurenghi G. Scotopic and fast mesopic microperimetry in eyes with drusen and reticular pseudodrusen. *Retina*. 2019;39:2378–2383.
24. Curcio CA, Messinger JD, Sloan KR, Mitra A, McGwin G, Spaide RF. Human chorioretinal layer thicknesses measured in macula-wide, high-resolution histologic sections. *Invest Ophthalmol Vis Sci*. 2011;52:3943–3954.
25. Jiang X, Shen M, Wang L, et al. Validation of a novel automated algorithm to measure drusen volume and area using swept source optical coherence tomography angiography. *Transl Vis Sci Technol*. 2021;10:11.
26. Schindelin J, Arganda-Carreras I, Frise E, et al. Fiji: an open-source platform for biological-image analysis. *Nat Methods*. 2012;9:676–682.
27. Sonoda S, Sakamoto T, Yamashita T, et al. Luminal and stromal areas of choroid determined by binarization method of optical coherence tomographic images. *Am J Ophthalmol*. 2015;159:1123–1131.e1.
28. Prakash YS, Smithson KG, Sieck GC. Application of the Cavalieri principle in volume estimation using laser confocal microscopy. *NeuroImage*. 1994;1:325–333.
29. Balaratnasingam C, Inoue M, Ahn S, et al. Visual acuity is correlated with the area of the foveal avascular zone in diabetic retinopathy and retinal vein occlusion. *Ophthalmology*. 2016;123:2352–2367.
30. Balaratnasingam C, Yannuzzi LA, Curcio CA, et al. Associations between retinal pigment epithelium and drusen volume changes during the lifecycle of large drusenoid pigment epithelial detachments. *Invest Ophthalmol Vis Sci*. 2016;57:5479–5489.
31. Faul F, Erdfelder E, Buchner A, Lang AG. Statistical power analyses using G*Power 3.1: tests for correlation and regression analyses. *Behav Res Methods*. 2009;41:1149–1160.
32. Bressler NM, Munoz B, Maguire MG, et al. Five-year incidence and disappearance of drusen and retinal pigment epithelial abnormalities. Waterman study. *Arch Ophthalmol*. 1995;113:301–308.
33. Sarks SH, Arnold JJ, Killingsworth MC, Sarks JP. Early drusen formation in the normal and aging eye and their relation to age related maculopathy: a clinicopathological study. *Br J Ophthalmol*. 1999;83:358–368.
34. Sadigh S, Cideciyan AV, Sumaroka A, et al. Abnormal thickening as well as thinning of the photoreceptor layer in intermediate age-related macular degeneration. *Invest Ophthalmol Vis Sci*. 2013;54:1603–1612.
35. Jones BW, Watt CB, Frederick JM, et al. Retinal remodeling triggered by photoreceptor degenerations. *J Comp Neurol*. 2003;464:1–16.
36. Marc RE, Jones BW, Watt CB, Vazquez-Chona F, Vaughan DK, Organisciak DT. Extreme retinal remodeling triggered by light damage: implications for age related macular degeneration. *Mol Vis*. 2008;14:782–806.
37. Strettoi E, Pignatelli V, Rossi C, Porciatti V, Falsini B. Remodeling of second-order neurons in the retina of rd/rd mutant mice. *Vision Res*. 2003;43:867–877.
38. Li M, Dolz-Marco R, Huisingh C, et al. Clinicopathologic correlation of geographic atrophy secondary to age-related macular degeneration. *Retina*. 2019;39:802–816.
39. Pfau M, von der Emde L, Dysli C, et al. Determinants of cone and rod functions in geographic atrophy: AI-based structure-function correlation. *Am J Ophthalmol*. 2020;217:162–173.
40. Sassmannshausen M, Zhou J, Pfau M, et al. Longitudinal analysis of retinal thickness and retinal function in eyes with large drusen secondary to intermediate age-related macular degeneration. *Ophthalmol Retina*. 2021;5:241–250.
41. Vogl WD, Bogunovic H, Waldstein SM, Riedl S, Schmidt-Erfurth U. Spatio-temporal alterations in retinal and choroidal layers in the progression of age-related macular degeneration (AMD) in optical coherence tomography. *Sci Rep*. 2021;11:5743.
42. Mullins RF, Johnson MN, Faidley EA, Skeie JM, Huang J. Choriocapillaris vascular dropout related to density of drusen in human eyes with early age-related macular degeneration. *Invest Ophthalmol Vis Sci*. 2011;52:1606–1612.
43. Mullins RF, Schoo DP, Sohn EH, et al. The membrane attack complex in aging human choriocapillaris: relationship to macular degeneration and choroidal thinning. *Am J Pathol*. 2014;184:3142–3153.
44. Bhutto I, Lutty G. Understanding age-related macular degeneration (AMD): relationships between the photoreceptor/retinal pigment epithelium/Bruch's membrane/choriocapillaris complex. *Mol Aspects Med*. 2012;33:295–317.
45. Borrelli E, Souied EH, Freund KB, et al. Reduced choriocapillaris flow in eyes with type 3 neovascularization and age-related macular degeneration. *Retina*. 2018;38:1968–1976.
46. Curcio CA, Zanzottera EC, Ach T, Balaratnasingam C, Freund KB. Activated retinal pigment epithelium, an optical coherence tomography biomarker for progression in age-related macular degeneration. *Invest Ophthalmol Vis Sci*. 2017;58:BIO211–BIO226.
47. Nassisi M, Baghdasaryan E, Borrelli E, Ip M, Sadda SR. Choriocapillaris flow impairment surrounding geographic atrophy correlates with disease progression. *PLoS One*. 2019;14:e0212563.
48. Nassisi M, Tepelus T, Corradetti G, Sadda SR. Relationship between choriocapillaris flow and scotopic microperimetry in early and intermediate age-related macular degeneration. *Am J Ophthalmol*. 2021;222:302–309.
49. Ledesma-Gil G, Fernandez-Avellaneda P, Spaide RF. Swept-source optical coherence tomography angiography image compensation of the choriocapillaris induces artifacts. *Retina*. 2020;40:1865–1872.
50. Keenan TD, Klein B, Agron E, Chew EY, Cukras CA, Wong WT. Choroidal thickness and vascularity vary with disease severity and subretinal drusenoid deposit presence in nonadvanced age-related macular degeneration. *Retina*. 2020;40:632–642.
51. Chung SE, Kang SW, Lee JH, Kim YT. Choroidal thickness in polypoidal choroidal vasculopathy and exudative age-related macular degeneration. *Ophthalmology*. 2011;118:840–845.
52. Dolz-Marco R, Balaratnasingam C, Gattoussi S, Ahn S, Yannuzzi LA, Freund KB. Long-term choroidal thickness changes in eyes with drusenoid pigment epithelium detachment. *American Journal of Ophthalmology*. 2018;191:23–33.
53. Agrawal R, Wei X, Goud A, Vupparaboina KK, Jana S, Chhablani J. Influence of scanning area on choroidal vascularity index measurement using optical coherence tomography. *Acta Ophthalmol*. 2017;95:e770–e775.
54. Sallo FB, Rechtman E, Peto T, et al. Functional aspects of drusen regression in age-related macular degeneration. *Br J Ophthalmol*. 2009;93:1345–1350.
55. Curcio CA, Millican CL, Allen KA, Kalina RE. Aging of the human photoreceptor mosaic: evidence for selective vulnerability of rods in central retina. *Invest Ophthalmol Vis Sci*. 1993;34:3278–3296.
56. Curcio CA. Photoreceptor topography in ageing and age-related maculopathy. *Eye (Lond)*. 2001;15:376–383.
57. Parisi V, Ziccardi L, Costanzo E, et al. Macular functional and morphological changes in intermediate age-related maculopathy. *Invest Ophthalmol Vis Sci*. 2020;61:11.

Investigative Ophthalmology & Visual Science

58. Chen C, Wu L, Wu D, et al. The local cone and rod system function in early age-related macular degeneration. *Doc Ophthalmol*. 2004;109:1–8.
59. Huang S, Wu D, Jiang F, et al. The multifocal electroretinogram in age-related maculopathies. *Doc Ophthalmol*. 2000;101:115–124.
60. Hood DC. Assessing retinal function with the multifocal technique. *Prog Retin Eye Res*. 2000;19:607–646.
61. Lee AY, Lee CS, Blazes MS, et al. Exploring a structural basis for delayed rod-mediated dark adaptation in age-related macular degeneration via deep learning. *Transl Vis Sci Technol*. 2020;9:62.
62. Pondorfer SG, Wintergerst MWM, Gorgi Zadeh S, et al. Association of visual function measures with drusen volume in early stages of age-related macular degeneration. *Invest Ophthalmol Vis Sci*. 2020;61:55.
63. Wu Z, Luu CD, Hodgson LAB, et al. Using microperimetry and low-luminance visual acuity to detect the onset of late age-related macular degeneration: a LEAD study report. *Retina*. 2021;41:1094–1101.
64. Wu Z, Luu CD, Hodgson LA, et al. Examining the added value of microperimetry and low luminance deficit for predicting progression in age-related macular degeneration. *Br J Ophthalmol*. 2021;105:711–715.

Investigative Ophthalmology & Visual Science